Quantitative Analysis of Magnetization Transfer by Phase Sensitive Method in Knee Disorder

Moon-Hyun Yoon[1], Mi-Sook Sung[2], Chang-Sik Yin[3], Heung-Kyu Lee[4], Bo-Young Choe[1]

Magnetization Transfer (MT) imaging generates contrast dependent on the phenomenon of magnetization exchange between free water proton and restricted proton in macromolecules. In biological materials in knee, MT or cross-relaxation is commonly modeled using two spin pools identified by their different T2 relaxation times. Two models for cross-relaxation emphasize the role of proton chemical exchange between protons of water and exchangeable protons on macromolecules, as well as through dipole-dipole interaction between the water and macromolecule protons. The most essential tool in medical image manipulation is the ability to adjust the contrast and intensity. Thus, it is desirable to adjust the contrast and intensity of an image interactively in the real time. The proton density (PD) and T2-weighted SE MR images allow the depiction of knee structures and can demonstrate defects and gross morphologic changes. The PD- and T2-weighted images also show the cartilage internal pathology due to the more intermediate signal of the knee joint in these sequences. Suppression of fat extends the dynamic range of tissue contrast, removes chemical shift artifacts, and decreases motion-related ghost artifacts. Like fat saturation, phase sensitive methods are also based on the difference in precession frequencies of water and fat. In this study, phase sensitive methods look at the phase difference that is accumulated in time as a result of Larmor frequency differences rather than using this difference directly. Although how MT work was given with clinical evidence that leads to quantitative model for MT in tissues, the mathematical formalism used to describe the MT effect applies to explaining to evaluate knee disorder, such as anterior cruciate ligament (ACL) tear and meniscal tear. Calculation of the effect of the effect of the MT saturation is given in the magnetization transfer ratio (MTR) which is a quantitative measure of the relative decrease in signal intensity due to the MT pulse.

Index words : Magnetization transfer (MT), fat saturation, phase sensitive method, ACL tear, meniscal tear, magnetization transfer ratio (MTR)

JKSMRM 10:98-107(2006)

[1]Department of Biomedical Engineering, College of Medicine, The Catholic University of Korea, Seoul, Korea
[2]Department of Radiology, College of Medicine, The Catholic University of Korea, Holy Family Hospital, Gyeunggi-Do, Korea
[3]Department of Acupuncture, CHA Biomedical Center, College of Medicine, Pochon CHA University, Korea
[4]ISOL Technology, 203 Neungpyeong-Ri, Opo-Eub, Gwangju-Si, Gyeonggi-Do, Korea
This study was presented at the 2006 World Congress of Medical Physics and Biomedical Engineering, Seoul COAX, Korea
Received; October 20, 2006, acceepted; December 1, 2006
Address reprint requests to : Bo-Young Choe, PhD, Department of Biomedical Engineering, Kangnam St. Mary's Hospital, College of Medicine, The Catholic University of Korea, 505 Banpo-dong, Seocho-gu, Seoul 137-040, Korea
Tel. 82-2-590-2427 Fax. 82-2-590-2425 E-mail: bychoe@catholic.ac.kr

Introduction

The many tissue parameters that can be measured by magnetization transfer imaging (MTI) methods have the potential to provide physiologic information about the repair or transplant as well. Because contrast is a measurement of the difference in signal between two regions, a measurement of contrast is independent of any arbitrary image scale factor. Contrast is usually defined as the signal difference divided by the average signal:

Contrast = 2(S1-S2) / (S1 + S2) [1]

The signal difference normalized to a measurement of the random noise is dimensionless and independent of any image gain factors as long as the noise is measured in the same units as the signal. An ideal MT contrast should provide accurate assessment of cartilage thickness, demonstrate morphologic changes of the cartilage surface, demonstrate internal cartilage signal changes, and allow evaluation of the subchondral bone for signal abnormalities. However, parallel to the development of a physical model for MT has been the development of imaging application that takes advantage of MT dependent contrast (MTC). Imaging using MTC was first demonstrated by Wolff and Balaban (1) in rabbit kidney using continuous-wave (CW) off-resonance irradiation to partially saturate the restricted pool. Nowadays, since CW irradiation is generally not available for clinical MRI scanners, the majority of human MT imaging has been performed using shaped off-resonance RF pulses (2 - 4) or short intense on-resonance binomial RF pulses (5). In either case the pulses are designed to selectively saturate (at least partially) the short T2 semi-solid spins without any direct effect on the liquid components (6, 7). In an attempt to isolate MT effects, acquisitions are often performed with and without 1H saturation pulses to compute ratio or percent difference images. Calculation of the effect of the MT saturation is given in the magnetization transfer ratio (MTR) that is found by the following equation:

$$MTR = (M_0 - M_s) / M_0 = 1 - M_s / M_0 \quad [2]$$

where M0 represents the signal intensity when no saturation pulses are applied and Ms the corresponding intensity with MT saturation on. The parameters that determine the MTR values can be classified in three groups: tissue properties, system parameters and data processing. Tissue properties exhibit different degrees of magnetization transfer. However, the uncertain relationship between tissue properties and MTR complicates the process of standardization and it is not yet possible to predict the behavior of individual tissues in different MR systems. Low MTR can arise from several physical (tissue) properties: for example a reduced capacity of the macromolecules in knee tissue to exchange magnetization with the surrounding water molecules or a decreased amount of macromolecules. The MTR is a semi-quantitative measure of the relative decrease in signal intensity due to the MT pulse. The use of pulsed irradiation to generate MT contrast requires further refinement of the physical model. A number of authors have described analytic methods for computing the transient behavior of binary spin model in response to step changes in irradiation (8, 9). The absorption line shape of the restricted protons determines the degree of saturation of the restricted protons. This absorption line shape can be taken as a Lorentzian, according to the Bloch equations. The frequency offset influences the degree of saturation due to the absorption line shapes of both the free and the restricted protons, which are frequency dependent. It should be noted that some absorption line shapes are asymmetric with respect to the centre, therefore the standard offset in all sequences is chosen to be on the negative side of the spectrum (10).

Fat suppression method takes advantage of the difference in the Larmor frequencies of fat and water. If the field is homogeneous enough, a narrow band RF pulse can be used to tip either species into the transverse plane without influencing the other pulse. A 90 °RF pulse tuned to the resonance frequency of fat is applied to tip the bulk magnetization vector from fat into the transverse plane. Fat saturation (FATSAT) is only a selective pulse sequence hence it tips down all fat magnetization regardless of the fat's location in the object. This is the FATSAT part of the sequence, and is followed by the spatially selective imaging sequence to obtain signal from the remaining water nuclei. Inversion-recovery (IR) imaging is independent of magnetic field inhomogeneities. This method takes advantage of the differences between T1 tissue relaxation times of fat and water by using an inversion-recovery sequence. An inversion pulse tips the

magnetization vector 180 ° or simply inverts the longitudinal magnetization. Fat has a shorter TI relative to water, thus recovers faster when an inversion pulse is applied. After a time delay, TI, all of the magnetization from fat will be in the transverse plane or simply Mz for fat will be zero, while most of the water magnetization is still pointing in the negative z-axis direction. Application of a 90 ° RF pulse at this point will result in data with null fat signal. The null point for tissues in the finite TR case is given by (11)

$$TI = T_1 \cdot 2 / (1 + e^{-TR/T1}) \quad [3]$$

In comparison to a conventional spin echo where tissues with a short T1 are bright due to faster recovery, fat signal is reversed or darkened. Because body fluids have both a long T1 and a long T2, it is evident that STIR offers the possibility of extremely sensitive detection of body fluid. This is of course, only true for stationary fluid such as edema, as the MR signal of flowing fluids is governed by other factors.

Materials and Methods

Magnetization transfer

Magnetization transfer (MT) imaging is an MRI technique that generates contrast dependent on the phenomenon of magnetization exchange between 'free water' protons and protons that are 'restricted' in macromolecules. This technique makes it possible to image 1H nuclei (protons) that are bound in semi-solids, such as proteins. The relaxation decay time of these materials is too short to image directly and therefore this indirect imaging technique is a perfect way to provide insight in the characteristics of these semisolid materials. Magnetization transfer imaging uses an off-resonance RF pulse to saturate bound hydrogen spins that are bound to collagen molecules. The saturated bound spins exchange with free water spins. Several studies have demonstrated that the magnetization transfer effect can be used to discriminate among articular cartilage, adjacent joint fluid, and inflamed synovium. (12 - 14)

The method uses two data sets, one acquired with magnetization transfer saturation on and one with it off. Unfortunately, patient motion occurring between these acquisitions can result in subtraction artifacts. Also, the SNR of the subtraction image is generally poorer than that of the component images because the signals cancel, whereas the noise is additive. If a different percentage of collagen is present in the repair tissue than in the adjacent cartilage, a change in the amount of magnetization transfer might be seen with this technique (15)

Method to image cartilage

Reasonable morphologic evaluation of cartilage and chondral pathology is achieved with (1) proton-density (PD) and T2-weighted fast spin echo (FSE) .PD-w and T2-w also show cartilage internal pathology due to the more intermediate signal of the cartilage in these sequences.

Immediately after an RF excitation, water and fat are aligned in the transverse plane, but they start to precess at different frequencies. The phase angle Φ between fat and water magnetizations changes in time, which can be expressed as

$$\Phi = 2¼t \cdot \Delta f_{wf} \quad [4]$$

when the phase difference is an odd multiple of ¼, water and fat point in opposite directions. The resulting signal will be minimum because out-of-phase magnetization vectors cancel each other. When the phase difference is an even multiple of ¼, water and fat points in the same directions or they are in-phase. In this case, the resulting signal will be maximum. Together with the relaxation effects, an oscillatory signal behavior is observed, especially in gradient echo sequences as shown in Figure. 1.

A refocusing RF pulse would correct not only for the field inhomogeneity but also phase cancellation due to chemical shift. Like fat saturation, phase sensitive techniques are also based on the difference in precession frequencies of water and fat. However, rather than using this difference directly, phase sensitive methods look at the phase difference that is accumulated in time as a result of Larmor frequency differences. The 2-point Dixon method (2PD) can be achieved within reasonable scan times while retaining a high spatial resolution (16). The method employs an acquisition of a pair of images with fat and water magnetizations aligned in-phase and out-of-phase (opposed-phase), respectively. Addition or subtraction of these images will result in either water or fat images. The first of the two images is obtained using a conventional SE sequence. The second image is acquired using the same sequence with a change in the

timing of the 180 ° refocusing pulse. FIG. 2 shows the timing diagram of the opposed-phase data acquisition. The time location of the conventional SE sequence used in the first image is shown with dashed lines. Right after the excitation fat and water magnetizations are in phase, however, they start to dephase as they precess at different Larmor frequencies. Accumulated phase dispersion until the 180 ° refocusing pulse is applied is given by

$$\Phi(TE - T_{off}) = 2¼ \Delta f_{wf} (TE - T_{off}) \quad [5]$$

where Toff is the correct timing offset. Once the refocusing pulse is applied, faster precessing water molecules will fall behind and experience a phase lag of $\Phi(TE - T_{off})$. Because the angular speed of precession is constant, it would take exactly the same amount of time to rewind the phase difference. At t = 2(TE?Toff), fat and water magnetizations are aligned in phase. From this point, the phase dispersion starts to build up again. The duration of this time window (Tphase) to build up a phase dispersion of ¼ radians is given by

$$T_{phase} = 2TE - 2 (TE - T_{off}) = 2 T_{off} \quad [6]$$

With this timing adjustment, the fat magnetization is out of phase at the time TE of the signal read-out. Because chemical shift is proportional to B0, Toff is inversely related to the field strength. For example, Toff is only 1.1 msec at 1.5 Tesla to achieve an opposed phase effect (17). Only the opposed-phase image is obtained with different echo times, which is characterized by decreased signal at tissue boundaries of the fat and water interface. The voxels containing both fat and water appear dark as their signals destructively interfere. The method works best in regions where fat and signal contributions are similar. In tissues that contain predominantly lipid or water, signal reduction is minimal. The problem with this technique is that there is no way to tell whether the

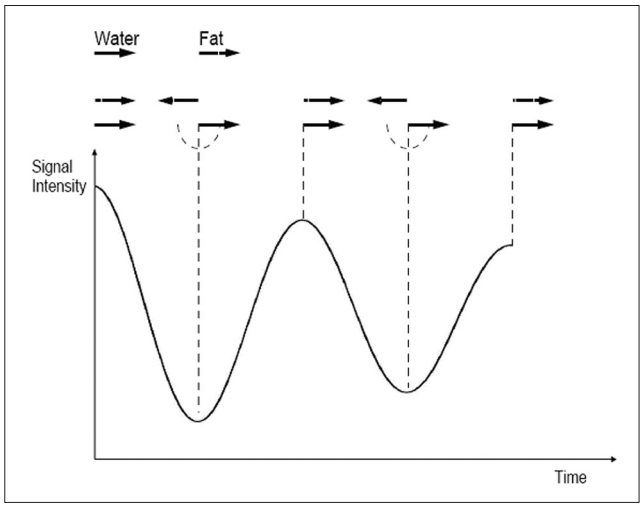

Fig. 1. Phase-cancellation artifact as a result of chemical shift. When the water and fat magnetizations are out of phase, minimum signal intensity is observed. When they are in phase, maximum intensity is observed. When they are in phase, maximum intensity is obtained under the existence of relaxation.

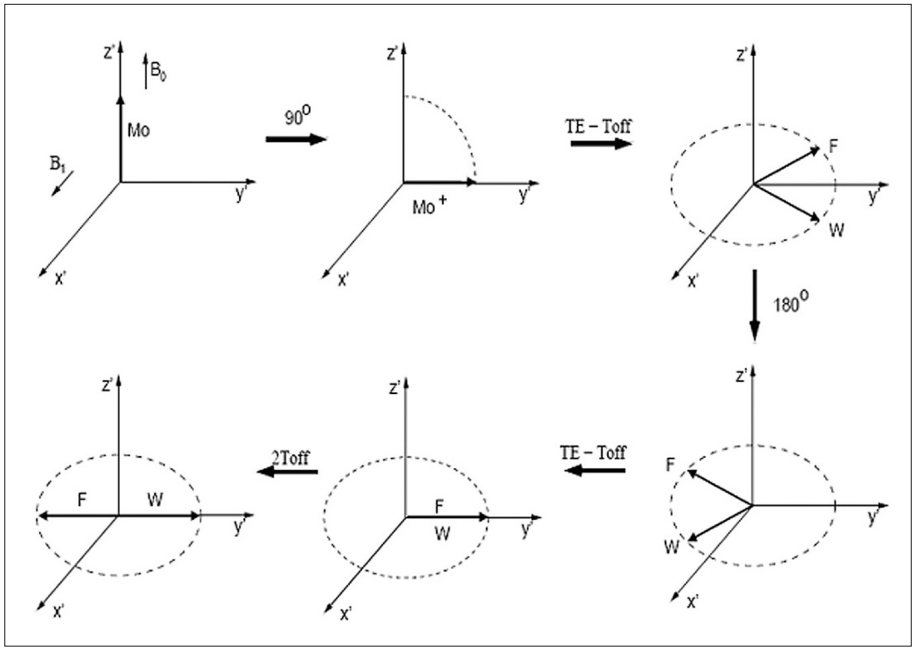

Fig. 2. Out of phase spin echo generation. Magnetization vectors for water (W) and fat (F) are in phase, initially. By simply equating the phase offset that is accumulated to ¼ radians, T_{off} for opposed-phase imaging is found as $2¼ \Phi f_{wf} (2T_{off}) = ¼ => T_{off} = ¼ \Phi f_{wf}$.

boundary voxels are mostly fat or water. Furthermore, it can be difficult to detect small tumors embedded in fat (18) because the signal from the tumor might be nulled by the signal from the surrounding adipose tissue. On the other hand, opposed-phase imaging is fast, simple, and available on commercial MR systems.

Fat Saturation: A 90 °RF pulse tuned to the resonance frequency of fat is applied to tip the bulk magnetization vector from fat into the transverse plane. One should keep in mind that fat saturation is only spectrally selective, hence it tips down all fat magnetization regardless of the fat's location in the object.

Inversion recovery doubles the distance spins will recover, allowing more time for T1 differences. A 180° preparation pulse inverts the net magnetization to the negative longitudinal magnetization prior to the 90° excitation pulse. This specialized application of the Inversion Recovery pulse sequence set the inversion time (TI) of the sequence at 0.69 times the T1 of fat. The T1 of fat at 1.5T is approximately 250 with a null point of 170 ms while at 0.5T its 215 with a 148 ms null point. At the moment of excitation, about 120 to 170 ms after the 180° inversion pulse (depending of the magnetic field) the magnetization of the fat signal has just risen to zero from its original, negative, value and no fat signal is available to be flipped into the transverse plane. The most attractive property of fat saturation is that, because it only modifies the fat signal, it can be applied to virtually any sequence. Because of the T1 relaxation, fat signal recovers; thus only a limited time is available (approx. 100 msec) for imaging. Repeating the fat saturation pulse is a solution, but fat saturation pulses consume a considerable amount of time, reducing the already limited time available for image acquisition.

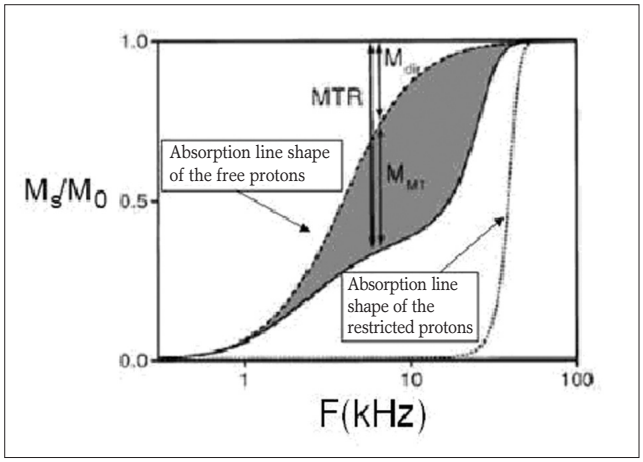

Fig. 3. Graph of the contributions of the direct effect and the MT effect to the M_s/M_0 value at different frequency offsets.

Method to process MTR data

The MR signal is a complex function of proton density, T2, T1, flow, diffusion and other sample properties. The signal intensity in an image is also influenced by the variance of RF pulses and gradients. The use of different RF pulse sequences creates different appearance for various tissues on the MR image. For off-resonance saturation transfer techniques, unwanted direct saturation effects play an important role, because off-resonance pulses also saturate the free pool directly. This direct saturation is caused by the fact that - although the free protons have a very narrow absorption peak - there will always be some saturation in the 'tail' of the absorption line shape. This can be seen from FIG.3 in which M_s/M_0 is graphed versus frequency offset on a log scale. The M_s/M_0 is composed of the direct saturation of the free pool (Mdir) and a contribution due to transfer effects (MMT). The striped line for the direct effect reflects the (Lorentzian) lineshape of the free protons.

The composition of the MTR due to these two effects could be written as:

$$MTR = (M_0 - M_s)/M_0 = 1 - (M_{dir}/M_0 + M_{MT}/M_0) \quad [7]$$

In qualitative imaging it is necessary to distinguish between MT and direct effect, which often images with contrast generated by both MT and the direct effect are used (19, 20). The direct effect may be reduced by either increasing the frequency offset or reducing the amplitude of the MT saturation pulse. Calculation of MTR for individual pixels depends on registration of unsaturated and saturated images. A shift of 1 mm or less due to patient motion may be enough to render invalid the calculated MTR value, especially where image intensity varies over a small distance (e.g. with small lesions or at tissue boundaries). At tissue interfaces (e.g. the entire joint structure, including the cartilage, menisci, synovial tissue, and ligaments), image pixels may sample a mixture of tissue, resulting in partial volume effect with MTR values somewhere between the values of the individual tissues. Such effects are variable and will be reduced, but never fully eliminated, by higher resolution imaging.

Jim™ is a medical image display package that allows easy viewing and analysis of Magnetic Resonance. For a magnetization transfer ratio (MTR) calculation, you will use two images (the images without and with off-resonance saturation pulses). For a simple image subtraction you will be working with two images. Performing an MTR calculation refers to the image without the saturation pulses as "M0" and the image with saturation pulses as "Ms". If you wish, alter the name in the Name field at the right hand side of each input image. Each input image must be of the same dimensionality (i.e., the same number of slices, and rows and columns within the slice). The algebra formula (e.g., I= $100(M_0 - M_s)/M0$ works through every pixel in the set of input images, and applies the formula to produce a single output image derived from a combination of the input images

Results

Some different images (PD-, T2-, and MTR-image) of an ACL tear and meniscal tear in patient's knee are shown in FIG. 4. It is clear that the contrast is very different for these four different images. Abnormalities in the knee are very clear on the MTR image. Performing an MTR calculation refers to the image (Fig. 4A, 5A) without the saturation pulses as "M0", and the image (Fig. 4B, 5B) with saturation pulses as "Ms". Fat saturation is the process of utilizing specific MRI parameters to remove the deleterious effects of fat from the resulting images. When deciding on the optimal short T1 time, factors to be considered include not only the main field strength, but also the tissue to be suppressed and the anatomy. In comparison to a conventional spin echo where tissues with a short T1 are bright due to faster recovery, fat signal is reversed or darkened. Because body fluids have both a long T1 and a long T2, it is evident that short T1/tau inversion

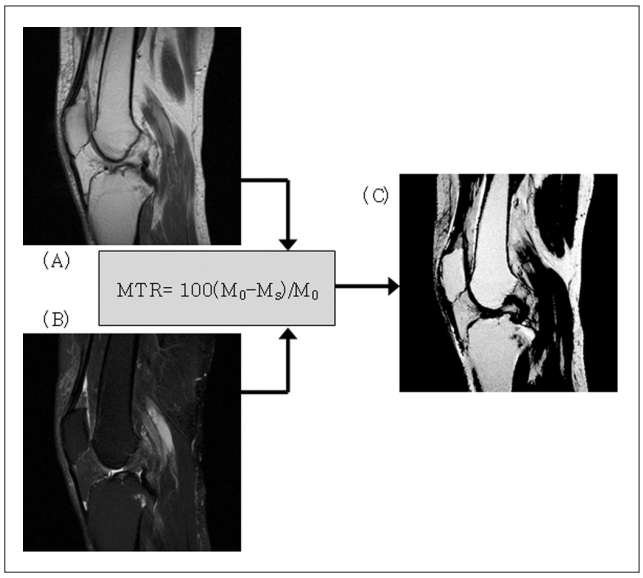

Fig. 5. (A) Sagittal spin echo proton density obtained from 55 year-old female. TR 2000 ms, TE 35 ms, NEX 3, ETL 3, and (B) Fat suppressed T2-weighted images obtained from TR 3215.08 ms, TE 70ms, NEX 3, ETL 9. Anterior horn of medial meniscus is normal with triangular low signal intensity (short arrows). Posterior horn of the medial meniscus shows increased signal intensity with inferior articular extension, indicating the meniscal tear (arrows). (C) Composition of an MTR image of ACL tear patient from a PD weighted image without (M_0) and a T2 image with fat saturation (M_s).

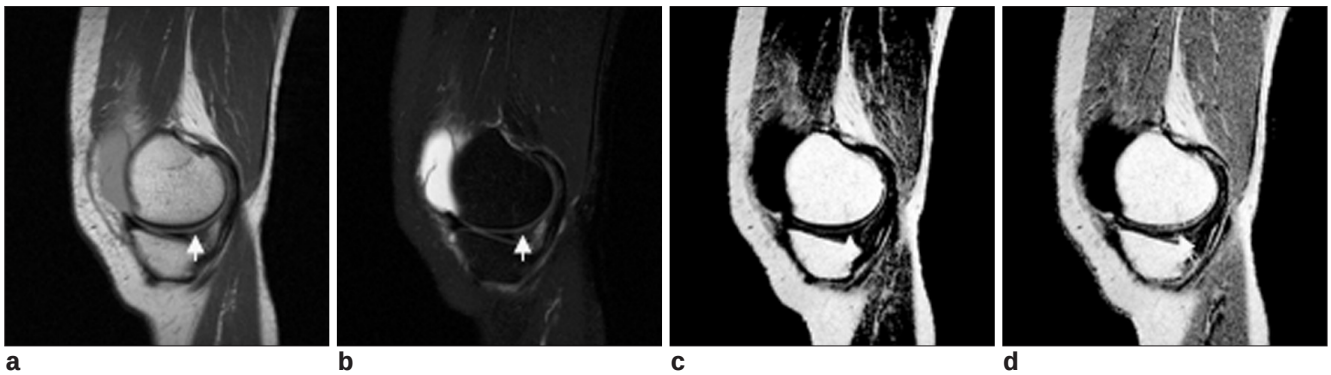

Fig. 4. (**a**) Sagittal spin echo proton density obtained from 56 year-old female. TR 2000 ms, TE 35 ms, NEX 3, Echo Train Length 3, and (**b**) fat suppressed T2-weighted image obtained from TR 3418.67 ms, TE 90ms, NEX 2, ETL 11. Anterior cruciate ligament shows increased signal intensity, indicating tear (arrow). (**c**) MTR image of bins 1% with threshold intensity; 120. (**d**) MTR image of bins 0.1% with threshold intensity; 150.

recovery (STIR) offers the possibility of extremely sensitive detection of body fluid. This is of course, only true for stationary fluid such as synovia, as the MR signal of flowing fluids is governed by other factors. There is only a small band of tissue where the fat protons are precessing at the frequency expected, resulting in frequency selective fat saturation working only in that area. This can be corrected by volume shimming or creating a more symmetrical volume being imaged with water bags. Even with their longer scan time and motion sensitivity, STIR sequences are often the better choice to suppress fat. STIR images (Fig. 4B, 5B) are also preferred because of the decreased sensitivity to field inhomogeneities, permitting larger fields of views when compared to fat suppressed images and the ability to image away from the isocenter. Fat suppression is the process of utilizing specific MRI parameters to remove the deleterious effects of fat from the resulting images with STIR and FAT SAT.

JimTM can display complex images - images where the real and imaginary parts are represented by separate 32-bit floating point values (interleaved). Magnitude displays the magnitude of the complex image. Phase displays the phase of the complex image (Fig. 4AB, 5AB). When the coordinate system of image dimensions is shown in pixels, pixel coordinates are always shown in integer values of pixel number. Pixel (1, 1) is at the top left of the image, and the column and row number increase to the right and downwards respectively. When the coordinate system of image dimensions is shown in millimeters, the origin (0, 0) is at the centre of the field-of-view, and the x and y values increase to the right and downwards respectively. A graph of vertical or horizontal intensity profiles are shown through an image slice. With a slice selected, the graph shows a plot of image intensity along a horizontal or vertical line through the image. In the Profile frame, the read-out at the bottom of the frame will show the location of the mouse pointer relative to the image slice, with the read out showing the row/column location in the image, the horizontal/vertical position within the row/column, and the intensity (I) at that position.

Discussion

MRI can be a valuable tool not only in evaluating the status of the ACL but also in assessing for associated abnormalities of internal derangement. The accuracy of MRI in the detection of acute ACL disruption ranges from 90% to 95%; however, it is slightly less accurate in depicting partial-thickness tears and chronic ACL-deficient knee conditions (21, 22). A thorough understanding of the normal MR appearance, signs of injury, and anatomical pitfalls of the meniscus is essential if one is to maximize diagnostic accuracy (23). MRI has evolved into a valuable tool for the preoperative evaluation of the menisci. Short TEs used for meniscal imaging can result in increased meniscal signal because of the magic angle phenomenon, when a part of the meniscus is oriented obliquely to the static magnetic field. This phenomenon is observed in the posterely to the static magnetic field. (24) The amplitude, shape and duration of the MT saturation pulse and the interpulse interval (duty cycle) determine the degree of saturation of both the free and restricted protons. A number of studies have addressed this issue for off-resonance pulsed saturation transfer imaging techniques. (25, 26). Most important determinant is the total energy of the MT pulse. The frequency offset influences the degree of saturation due to the absorption line shapes of both the free and the restricted protons, which are frequency dependent. It should be noted that some absorption line shapes are asymmetric with respect to the centre, therefore the standard offset in all sequences is chosen to be on the negative side of the spectrum (10). Other factors that always influence the signal intensity in MR imaging also determine the received MT signal. The fluid provides the hydraulic capacity for the pressurization of the tissue, whereas the fluid-filled solid network provides resistance to fluid flow, which slows tissue consolidation. The cause of the hydration changes is unclear but includes the loss of or damage to the solid matrix elements. The absorption line shape of the restricted protons (also shown in FIG. 3 as dotted line) determines the degree of saturation of the restricted protons. This absorption line shape can be taken as a Lorentzian, according to the Bloch equations. The problem with this approach is that it not uses the

knowledge of the biophysical properties of the tissue and specific details of the MR pulse sequence. Some of the biophysical knowledge and the MR parameters were taken into account (27). MTR can be used in several ways. MTR values can be obtained from individual lesions or discrete areas from the overall lesion population, the entire normal appearing cartilage or even the overall knee, thus assessing the microscopic and the macroscopic burdens of the disease together. However, there has been a discrepancy in the analysis of pulsed experiments with respect to generalizing the behavior of the restricted pool; the irradiation induced transition rate has either been assumed constant or time-varying (28, 29).

Because MTR seems to be a very unstable parameter to characterize magnetization transfer, many attempts have been made to find another more uniform parameter. Some investigators have attempted to quantify MT images by calculating a rate constant about fat saturation (30):

$$k_{SAT} = \frac{1}{T_{1SAT}}\left(1 - \frac{M_s}{M_0}\right) = \frac{1}{T_{1SAT}} = \cdot \text{MTR} \qquad [8]$$

in which T1sat is the time constant for the two pools to come to equilibrium. Although the algebra can always be performed, the rate constant ksat only has physical meaning if two physical conditions are satisfied: the macromolecular spins must be kept fully saturated and there should be no direct effect on the liquid spins. Because these conditions are not always satisfied, although it purports to be a constant of NMR dynamics, is only a phenomenological measure and is still not more than a semi-quantitative value (20). The parameters that determine the MTR values can be classified in tissue properties. The fact that different tissues exhibit different degrees of magnetization transfer provides the rationale for using these techniques. However, the uncertain relationship between tissue properties and MTR complicates the process of standardization and it is not yet possible to predict the behavior of individual tissues in different MR systems.

Conclusion

Investigation of physical basis of MTR and evaluation of the widely used fat saturation technique, as done in this study with an experimental and theoretical approach, can provide us more insight in the physical and technical basis of magnetization transfer imaging. A theoretical approach could provide the link between the measured signal intensity and the physical properties of the knee and the system parameters. In the future, this could be of considerable interest for the quantification of osteoarthritis in knee or shoulder.

Acknowledgment

This study was supported by a grant of the Seoul R&BD Program (10550), the Korea Health 21 R&D Project, Ministry of Health & Welfare, Republic of Korea (02-PJ3-PG6-EV07-0002) and a grant of the 2005 Nuclear R&D Plan Program, Ministry of Science & Technology, Korea.

References

1. Wolff SD, Balaban R S Magnetization transfer contrast (MTC) and tissue water proton relaxation in vivo. Magn Reson Med 1989;10(1):135-44
2. Pierce WB, Harms SE, Flamig DP, Griffey RH, Evans WP, Hagans JE. Three-dimensional gadolinium-enhanced MR imaging of the breast: Pulse sequence with fat suppression and magnetization transfer contrast. Radiology 1991;181:757-763
3. Schnall MD, Dougherty L, Outwater E, Dousset V. Technique for magnetization transfer imaging at 1.5T using steady state pulsed saturation. In Proceedings of the Tenth Annual Meeting of the ISMRM, San Francisco, USA, 1991;175
4. Schneider E, Prost RW, Glover GH. Pulsed magnetization transfer versus continuous wave irradiation for tissue contrast enhancement. J Magn Reson Imaging 1993;3(2):417-423
5. Pike GB, Glover GH, Hu BS, Enzmann DR. Pulsed magnetization transfer spin-echo MR imaging. J Magn Reson Imaging 1993;3(3):531-539
6. Graham SJ, Henkelman RM. Pulsed magnetization transfer imaging: evaluation of technique. Radiology 1999;212(3):903-910
7. Santyr GE, Kelcz F, Schneider E. Pulsed magnetization transfer contrast for MR imaging with application to breast. J Magn Reson Imaging 1996;6(1):203-212
8. Roell SA, Dreher W, Leibfritz D. A general solution of the standard magnetization transfer model. J Magn Reson 1998;132(1):96-101
9. Yeung HN, Adler RS, Swanson SD. Transient decay of longitudinal magnetization in hetrogeneous spin systems under selective saturation. IV. Reformulation of the spin-bath-model equations by the Redfield-Provotorov theory. J Magn Reson 1994;A 106:37-45
10. Silver NC, Barker GJ, Miller DH. Standardization of magnetization transfer imaging for multicenter studies. Neurology 1999;53(Suppl 3), S33-S39

11. Haacke EM, Brown RW, Thompson MR, Venkatesan R. Magnetic Resonance Imaging: Physical Principles and Sequence Design, John Wiley and Sons, Inc., USA, 1999.
12. Koskinen SK, Yla-Outinen H, Aho HJ. Magnetization transfer and spin lock MR imaging of patellar cartilage degeneration at 0.1 T. Acta Radiol 1997;38:1071-1075
13. Peterfy CG, van Dijke CF, Janzen DL. Quantification of articular cartilage in the knee with pulsed saturation transfer subtraction and fat-suppressed MR imaging: optimization and validation. Radiology 1994;192,:485-491
14. Seo GS, Aoki J, Moriya H, Karakida O. Hyaline cartilage: in vivo and in vitro assessment with magnetization transfer imaging. Radiology 1996;201:525-530
15. Lattanzio PJ, Marshall KW, Damyanovich AZ. Macromolecule and water magnetization exchange modeling in articular cartilage. Magn Reson Med 2000;44:840-851
16. Dixon WT. Simple Proton Spectroscopic Imaging. Radiology 1984;153:189-194
17. Bookstein FL. (1992) Morphometric Tools for Landmark Data : Geometry and Biology, Cambridge University Press, USA
18. Borrello JA, Chenevert TL, Meyer CR, Aisen AM, Glazer GM. Chemicalshift Based True Water and Fat Images: Regional Phase Correction of Modified Spinecho MR Images, Radiology 1987;164:531-538
19. Wolff SD, Balaban RD. Magnetization transfer contrast (MTC) and tissue water proton relaxation in vivo. Magn Reson Med 1989;10:135-144
20. Henkelman RM, Stanisz GJ, Graham SJ. Magnetization transfer in MRI: a review. NMR Biomed 2001;14:57-64.
21. Ha TP, Liu KC, Beaulieu CF. Anterior cruciate ligament injury: fast spin-echo MR imaging with arthroscopic correlation in 217 examinations. AJR 1998;170:1215-1219.
22. Mink JH, Levy T, Crues JVI. Tears of the anterior cruciate ligament and menisci of the knee: MR imaging evaluation. Radiology 1988;167:769-774.
23. De Smet AA, Tuite KJ, Norris MA, Swan JS. MR diagnosis of meniscal tears: analysis of causes of errors. AJR Am J Roentgenol 1994;163:1419-1423
24. Peterfy CG, Janzen DL, Triman PFJ, Van Dijke CF, Pollack M, Genaat HK. Magic angle phenomenon: a cause of increased signal in the normal lateral meniscus on short-TE MR images of the knee. AJR Am J Roentgenol 1994;163:149-154
25. Pike GB. Pulsed magnetization transfer contrast in gradient echo imaging: a two pool analytic description of signal response. Magn Reson Med 1996;36:95-103
26. Berry I, Barker GJ, Barkhof F, Campi A, Dousset V, Franconi J, Gass A, Schreiber W, Miller DH, Tofts PS, Phil D. A multicenter measurement of magnetization transfer ratio in normal white matter. J Magn Reson Imaging 1999;9:441-446
27. Sled JG, Pike GB. Quantitative interpretation of magnetization transfer in spoiled gradient echo MRI sequences. J Magn Reson 2000;145:24-36
28. Roell SA, Dreher W, Leibfritz D. A general solution of the standard magnetization transfer model. J Magn Reson 1998;132(1):96-101
29. Adler RS, Yeung HY. Transient decay of longitudinal magnetization in heterogenous spin systems under selective saturation. III solution by projection operators. J Magn Res Series A 1993;104:321-330
30. Ropele S, Strasser-Fuchs S, Fazekas F. A comparison of magnetization tranfer ratio, magnetization tranfer rate, and the native relaxation time of water protons related to relapsingremitting multiple sclerosis. AJNR Am J Neuroradiol 2000;21:1885-1891

대한자기공명의과학회지 10:98-107(2006)

무릎 이상에 대한 자화전이 위상감각에 의한 정량분석법

[1]가톨릭대학교 의과대학 의공학교실, [2]방사선과학교실
[3]포천중문의대 차병원, [4]아이솔테크날로지

윤문현[1] · 성미숙[2] · 인창식[3] · 이흥규[4] · 최보영[1]

자화전이영상 (MTI)은 무릎의 연골조직, 활액, 연대 등에 있는 거대분자에 붙어 분자운동에 제한을 받은 수소와 비교적 자유로운 물 분자의 수소가 두 가지 자화 상태로 서로 교환되고 있는 상태에서 한쪽 자화상태를 RF 펄스를 사용하여 포화시키면 다른 자화 상태가 교환 상황에 따라 그 신호강도가 달라지면서 영상의 대조도를 이룬다. 교차이완은 수소의 T2 이완시간이 다르면서 생기는 두 스핀 풀로 모델화하여 물 분자와 거대분자 사이의 쌍극자들의 상호교환 뿐만 아니라 물분자와 거대분자의 수소 화학교환으로 설명된다. 이에 의학영상에서 가장 필수적 요소인 신호강도와 대조도를 조절하는 능력으로서 양성자 밀도와 T2 강조 무릎영상을 획득하여 비정상적 조직과 그 변화 위에 시퀀스와 더불어 무릎 조인트의 중간신호들에 의해 무릎 연골주위의 다른 조직과의 신호강도 차이를 더욱 높이기도 한다. 또한 지방억제 기술은 조직 대조도를 증대시키고 화학전이 인공물을 제거할 뿐 아니라 움직임과 관련한 고스트 인공물을 감소시킨다. 이와 같은 지방 포화억제는 위상감각 방법 (Phase Sensitive Method)에서 물과 지방의 세차운동 주파수에 차이를 나타낸다. 본 연구에서 위상감각 방법은 Larmor 주파수 차이를 직접 사용하기 보다는 그 주파수 차이 결과를 축적하여 생기는 위상 차이를 보고자 하였다. 자화전이영상이 어떻게 작동하는가는 무릎조직의 자화전이 (MT)에 대한 정량적 모델로 유도되는 임상적 증거에서 주어지지만 그 자화전이 효과를 설명하는 수학적 공식화는 전방 십자형 인대 (Anterior Cruciate Ligament)파열과 관절간연골 파열과 같은 무릎관절질환을 평가하는 데 적용하였고, 자화전이 포화 효과의 계산은 MT 펄스에 의한 신호강도에 상대적 감소를 정량적으로 측정하는 자화전이률에 의해 주어졌다.

통신저자 : 최보영, (137-040) 서울시 서초구 반포동 505번지, 가톨릭대학교 의과대학 의공학교실
Tel. (02) 590-2427 Fax. (02) 590-2425 E-mail: bychoe@catholic.ac.kr